Available online at www.sciencedirect.com

ScienceDirect

Indagationes Mathematicae 32 (2021) 33–54

indagationes mathematicae

www.elsevier.com/locate/indag

Special issue in memory of Hans Duistermaat

Normal resonances in a double Hopf bifurcation

Henk Broer[a], Heinz Hanßmann[b], Florian Wagener[c,*]

[a] *Bernoulli Institute for Mathematics, Computer Science and Artificial Intelligence, Rijksuniversiteit Groningen, 9747 AG Groningen, The Netherlands*

[b] *Mathematisch Instituut, Universiteit Utrecht, Postbus 80010, 3508 TA Utrecht, The Netherlands*

[c] *Center for Nonlinear Dynamics in Economics and Finance (CeNDEF), Amsterdam School of Economics, Universiteit van Amsterdam, Postbus 15867, 1001 NJ Amsterdam, The Netherlands*

Abstract

We introduce a framework to systematically investigate the resonant double Hopf bifurcation. We use the basic invariants of the ensuing $\mathbb{T}^1$-action to analyse the approximating normal form truncations in a unified manner. In this way we obtain a global description of the parameter space and thus find the organising resonance droplet, which is the present analogue of the resonant gap. The dynamics of the normal form yields a skeleton for the dynamics of the original system. In the ensuing perturbation theory both normal hyperbolicity (centre manifold theory) and KAM theory are being used.

Keywords: Hopf bifurcation; Resonances; Normal forms; Invariants; KAM theory

1. Introduction

A central question of the theory of dynamical systems is stability loss of equilibria. Consider dynamics that is described by a one-parameter family of vector fields

$$\dot{z} = h(z,\mu), \qquad z \in \mathbb{R}^m, \quad \mu \in \mathbb{R},$$

such that $z = 0$ is an equilibrium for $\mu = 0$, and such that the derivative $D_z h(0,0)$ is invertible. By the implicit mapping theorem there is a family of equilibria z_μ passing through 0. We may assume that $z_\mu = 0$ for μ close to 0, if necessary after shifting the variables.

* Corresponding author.
E-mail address: f.o.o.wagener@uva.nl (F. Wagener).

https://doi.org/10.1016/j.indag.2020.09.003

Hopf bifurcation. For these dynamics, the simplest stability loss scenario is a Hopf bifurcation. Under this scenario, the eigenvalues of $D_z h(0, \mu)$ are in the left hand complex half plane $\{\lambda : \mathrm{Re}\,\lambda < 0\}$ for $\mu < 0$, implying that the central equilibrium is asymptotically stable. For $\mu = 0$, a pair of eigenvalues is on the imaginary axis, and for $\mu > 0$, the pair has crossed into the right hand complex half plane and the equilibrium is unstable. For the moment simplifying the argument, if necessary by applying centre manifold theory [29], we restrict to the case $m = 2$.

To understand how the orbit structure has changed through this bifurcation, the family of vector fields is simplified, 'normalised', through successive co-ordinate changes, resulting in a 'normal form' representation

$$h(z, \mu) \;=\; h_{\mathrm{N}}(z, \mu) \;+\; h_{\mathrm{R}}(z, \mu) \tag{1}$$

of the dynamics. The normal form co-ordinate changes can transform away all terms in the Taylor expansion of h, up to any given order in z, excepting terms that are invariant under the action of the linear vector field $D_z h(0, 0)z\partial_z$. As the linear vector field generates a rotation group $\mathbb{T} = \mathbb{R}/\mathbb{Z}$, the normal form term $h_{\mathrm{N}}(z, \mu)$ is equivariant with respect to this group; the high order remainder term $h_{\mathrm{R}}(z, \mu)$ is not normalised and hence does not have to be equivariant.

The analysis then proceeds in two steps. First the high order remainder term h_{R} is dropped, and only the approximate dynamics of the 'normal form truncation' h_{N} is considered. After dividing out the rotational symmetry, the dynamics reduces to the one-dimensional radial vector field, whose equilibria form a curve in the product of reduced phase space and parameter space. Reinstating the angular variable shows that this curve corresponds to a surface C in the product of phase space and parameter space, invariant under the rotation group $\mathbb{T}$, such that a plane $\mu = \mu_0$ intersects C in one or more circles that are invariant under the dynamics of $\dot{z} = h_{\mathrm{N}}(z, \mu_0)$.

Generically, the surface C has only quadratic contact with the plane $\mu = 0$ at $(z, \mu) = (0, 0)$. If C lies in the region $\mu > 0$, close to the point of tangency, we have a supercritical Hopf bifurcation: for $\mu < 0$ the equilibrium is stable, and for $\mu > 0$ a family of stable invariant circles bifurcates from the equilibrium, which turns unstable. A subcritical Hopf bifurcation is obtained if C lies in the region $\mu < 0$: then for $\mu < 0$ there is a family of unstable invariant circles which shrinks down to the stable equilibrium at $\mu = 0$, and for $\mu > 0$ only an unstable equilibrium is left.

The second step of the analysis is to reinstate the high order remainder term h_{R} and to use results from perturbation theory [29] to show that the manifold C of invariant circles also persists in the original system.

This Hopf bifurcation scenario generalises in several directions. An equilibrium can be viewed as a 0-dimensional torus, and a circle as a 1-dimensional torus by representing it as the diffeomorphic image of $\mathbb{T}$. The invariant circles, or 1-tori, that are generated in the bifurcation can go through a Hopf bifurcation themselves: in that case we speak of a Hopf–Neĭmark–Sacker bifurcation. As eigenvalues of the linearisation determine the stability of an equilibrium, the stability of an invariant circle is determined by its Floquet exponents. Apart from that, the analysis runs largely parallel in both cases. A Hopf bifurcation of invariant 1-tori can generate invariant bifurcating 2-tori, which can bifurcate to 3-tori, and so on, giving rise to the celebrated Hopf–Landau–Lifschitz bifurcation cascade [30,35,36,47].

The technical treatment of higher dimensional invariant tori is complicated by the fact that these tori may have complex internal dynamics. The situation that is closest to equilibrium

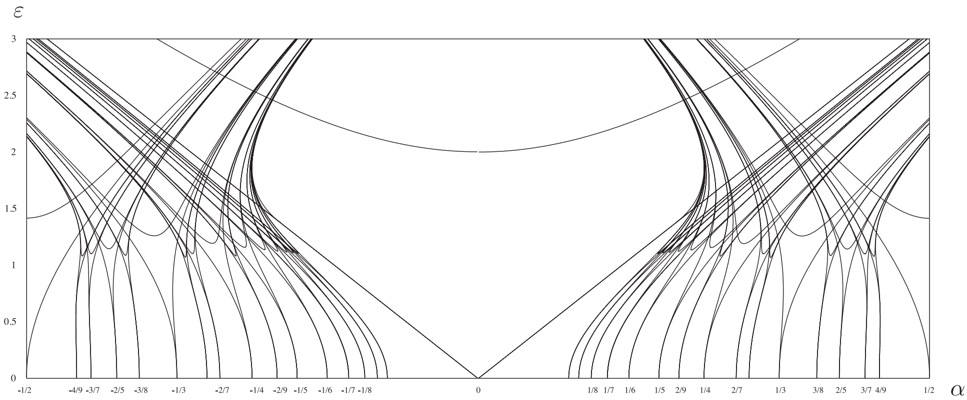

Fig. 1. Array of resonance tongues. Inside the resonance tongues the dynamics is resonant or phase locked. Intersection with a horizontal line results in an open and dense union of resonance gaps.

behaviour is obtained when the internal dynamics on the torus is quasi-periodic, that is, of the form

$$\dot{x} \;=\; \omega, \tag{2}$$

for $x \in \mathbb{T}^n$, where x is the vector of torus angles, and where the frequency vector $\omega \in \mathbb{R}^n$ is such that there is no relation $\langle k \mid \omega \rangle = 0$ with integer coefficients $k \in \mathbb{Z}^n$. Indeed, if the expression $\langle k \mid \omega \rangle$ is bounded away from 0 by Diophantine conditions, KAM theory can be invoked to show the persistence of these invariant tori.

Resonance. An important notion that comes up here is resonance. As an example consider the 2-torus $\mathbb{T}^2$ with a flow generated by (2). If the frequency vector ω has components ω_1 and ω_2 that have a rational relationship

$$\langle k \mid \omega \rangle \;=\; k_1\omega_1 \;+\; k_2\omega_2 \;=\; 0,$$

we speak of an (internal) resonance. The flow then consists of periodic orbits, foliating the torus. When no resonances are present each orbit fills the torus densely. In the resonant case the frequency ratio $\alpha = \omega_1/\omega_2$ is rational, while in the non-resonant case it is irrational. Both cases are dense in the α-axis; the set of frequency ratios satisfying a Diophantine condition, which is a strong form of non-resonance, has moreover full measure.

In this 2-dimensional context it is convenient to consider a Poincaré section transverse to the flow. The corresponding Poincaré mapping is a circle diffeomorphism. An interesting example to account for nonlinear effects is the Arnol'd family of circle diffeomorphisms given by

$$x \in \mathbb{T}^1 \;\mapsto\; x \;+\; 2\pi\alpha \;+\; \varepsilon \sin x, \tag{3}$$

where $\varepsilon \in \mathbb{R}$ is a perturbation parameter. In the (α, ε)-plane of parameters the values corresponding to resonant and non-resonant mappings are shown in Fig. 1.

Remarks.

- The interior of the resonance tongues constitutes an open and dense subset of the parameter plane and therefore is large in the topological sense.

- In the complement of the tongues the dynamics is quasi-periodic, each orbit densely filling the circle [24]. As it is straightforward to show that the measure of the resonance tongues tends to 0 as $\varepsilon \to 0$, it follows that the complement has positive measure tending to full measure.
- For $n > 2$ frequencies the situation is more complicated and partly still unknown.
- This geometric complexity will be met again in the sequel.

Double Hopf bifurcation. The double Hopf bifurcation is obtained if at bifurcation there are two pairs of imaginary eigenvalues, or two pairs of imaginary Floquet exponents. For this situation to occur stably in a family of vector fields, that is, occurring also in all families that differ from the given one by a small perturbation, we have to consider a family that depends on at least two parameters.

For simplicity we here restrict to the 4-dimensional case and first consider the non-resonant case, i.e., where there are no rational relations between the two normal frequencies. The linear dynamics $D_z h(0, 0) z \partial_z$ then generates a torus group $\mathbb{T}^2$. Normalisation and truncation yields two-dimensional reduced dynamics, as there are two radial variables, and there are now twelve different possible scenarios how the orbit structure around a double Hopf singular equilibrium can change as parameters change [27,34]. All of these scenarios feature a Hopf bifurcation from the central equilibrium to a 1-torus (or periodic orbit), and a second Hopf bifurcation from the 1-torus to a 2-torus. Depending on the scenario, there may be other subordinate bifurcations, in particular there are two of the twelve cases where also a third Hopf bifurcation from the 2-torus to a 3-torus occurs.

In this article, we discuss the resonant double Hopf bifurcation, that is a double Hopf bifurcation where there is at bifurcation an integer relation between the imaginary eigenvalues, or imaginary Floquet exponents. This concerns a normal resonance as opposed to the internal resonance met before. All of the complexity of the non-resonant double Hopf bifurcation is retained, but additionally there is the possibility that the internal dynamics of the 2-torus bifurcating off from the 1-torus changes from parallel to phase-locked.

Aim. The resonant double Hopf bifurcation has been investigated since the 1980s. The present paper introduces a framework that allows for a systematic investigation of the occurring phenomena. In all twelve cases of the double Hopf bifurcation subordinate bifurcations from a 1-torus to a 2-torus occur. In two of these cases also a bifurcation from a 2-torus to a 3-torus takes place: to fix thoughts we consider one of these cases. Our framework leads to a global picture of the parameter space. Here we meet 3-dimensional analogue of the Arnol'd tongues of Fig. 1. Transversal cuts with a plane result in what we call 'resonance droplets', the present analogue of the resonance gaps. Also we find a number of subordinate bifurcations of the double Hopf bifurcations not met before in the literature.

1.1. Setting

From now on we replace the central equilibrium point by an invariant n-torus. This puts the occurring Hopf bifurcations in the setting of quasi-periodic bifurcation theory [2,3,9]. Double Hopf bifurcations of n-dimensional tori in their simplest form occur in $n + 4$ dimensions. Therefore we consider a family of vector fields on an $(n + 4)$-dimensional manifold that leave invariant a family of conditionally periodic n-tori. Locally around the tori the dynamics is then of the form

$$\dot{x} = \omega(\mu) + O(z), \tag{4a}$$

$$\dot{z} \;=\; \Omega(\mu)\, z \;+\; O(z^2), \tag{4b}$$

with $x \in \mathbb{T}^n$ the vector of torus angles, $z \in \mathbb{R}^4$, and $\mu \in \mathbb{R}^s$ denoting the parameter. The symbol $O(z^k)$ represents a term of the form $R(x, z, \bar{z}, \mu)$ which is such that $\|R\|/\|z\|^k$ is bounded, uniformly in x, for z and μ in compact neighbourhoods of the origin of their respective spaces.

We assume the tori to be reducible to Floquet form and the double Hopf bifurcation to occur at $\mu = 0$. The eigenvalues of $\Omega = \Omega(\mu)$ are the Floquet exponents $\beta_j(\mu) \pm \mathrm{i}\alpha_j(\mu)$, $\alpha_j, \beta_j \in \mathbb{R}$ and $j = 1, 2$, of the invariant torus $\mathbb{T}^n \times \{0\}$.

For $\mu = 0$ the tori are at a double Hopf singularity if $\beta_j(0) = 0$ and $\alpha_j(0) \neq 0$ for $j = 1, 2$. Within this singularity, the normal frequencies $\alpha_j(0)$ are at normal–normal resonance if moreover

$$\ell_2\alpha_1(0) \;=\; \ell_1\alpha_2(0) \tag{5}$$

for some $0 \neq \ell = (\ell_1, \ell_2) \in \mathbb{Z}^2$. The aim of this article is to study the dynamics of the family (4) near such resonances.

The normal linear part of (4) is obtained by truncating the $O(z)$ and $O(z^2)$ terms in (4a) and (4b), respectively. The flow of this normal linear part is equivariant with respect to a $\mathbb{T}^n \times \mathbb{T}^2$ action, and in the resonant case (5) the symmetry group is even larger (the symmetry group is maximal in the case $\alpha_1(0) = \alpha_2(0) = 0$, which we do not consider further). The aim of normal form theory is to push the symmetry to higher order terms by successive transformations, compare with [27]. In the non-resonant case the entire $\mathbb{T}^n \times \mathbb{T}^2$ symmetry is inherited by the normalised dynamics. However, in the present normal–normal resonant case the normalised terms only inherit a $\mathbb{T}^n \times \mathbb{T}^1$ symmetry.

We apply finitely many normalising transformations in order to obtain a $\mathbb{T}^n \times \mathbb{T}^1$ symmetric truncation. In particular, the coefficients of monomials in z in the truncation are x-independent. In the truncated system the normal dynamics is decoupled from the internal dynamics, and it retains a $\mathbb{T}$ symmetry. After reducing this out, a three-dimensional system remains. Equilibria of the reduced system correspond to either n-dimensional or $(n + 1)$-dimensional invariant tori in the normal form truncation. The full system is a small perturbation of this truncation; to assess the impact of the higher order remainder terms, we invoke both normal hyperbolicity and KAM theory.

In (5) we may assume that $0 < \ell_1 \leq \ell_2$ and $\alpha_j(0) > 0$, $j = 1, 2$, if necessary by relabelling the frequencies and scaling the variables. We restrict to weak resonances: these are resonances where in (5) we have $0 < \ell_1 < \ell_2$: this rules out the strongly resonant case $\ell = (1, 1)$.

Remarks.

- Instead of starting in $n + 4$ dimensions we could also take as starting point a family of vector fields on an $(n + m)$-dimensional manifold. However, our first step would then be to split the normal spectrum of the bifurcating n-torus into the 4 purely imaginary eigenvalues $\pm\mathrm{i}\alpha_1(0)$, $\pm\mathrm{i}\alpha_2(0)$ and the remaining $m-4$ hyperbolic eigenvalues and to then perform a restriction to the resulting $(n + 4)$-dimensional normally hyperbolic invariant manifold on which we have the situation sketched above. We note that this procedure generically leads to a finitely differentiable system.
- We generally assume our systems to be real analytic, which facilitates the application of KAM theory. However, for applications on centre manifolds finitely differentiable versions of KAM theory are available [9,11,55].

- One of the improvements of normalisation theory in the analytic setting is that the remainder term can be made exponentially small [7,8,23,31,41] in the perturbation parameter. In the finitely differentiable case this would be only polynomially small.

1.2. Previous work

The resonant double Hopf bifurcation has already been studied by many authors. The strong 1:1 resonance, to which we do not contribute, has been studied in [25,26,43,49]. Of the weak resonances, the 1:2 resonance has gotten the most attention [32,33,37,38,40,45,52]; next to it, the 1:3 resonance [37,40] and the 2:3 resonance [44,46] have been investigated as well. For the Hamiltonian Hopf bifurcation, see [6,28].

Most previous work has been on the case $n = 0$ where the central torus reduces to an equilibrium that has two (normal) frequencies. We therefore also speak of 1-dimensional invariant tori instead of periodic orbits. The non-resonant case where only $\beta_1(0) = \beta_2(0) = 0$, but $\alpha_1(0)$ and $\alpha_2(0)$ do not satisfy (5) for any $0 \neq \ell \in \mathbb{Z}^2$, has a $\mathbb{T}^2$ symmetry instead of a $\mathbb{T}^1$ symmetry in the normal forms. Reduction leads to a 2-dimensional basis system and the dynamics of this 2-dimensional normal form was already laid out in [27]. However, it took until [39] for a formal proof of persistence of the resulting invariant tori under perturbation from the normal form back to the original system.

To summarise the literature on the weakly resonant case (again mostly concerning the case $n = 0$), it is convenient to call 'resonance droplet' the part of parameter space for which 1-dimensional invariant tori with non-zero amplitudes exist. This corresponds for instance with the 'mixed modes' situation of Knobloch and Proctor [32]. They made an extensive local study of that part of the boundary of the resonance droplet of the 1:2 resonant double Hopf bifurcation where a 1-dimensional torus bifurcates to a 2-dimensional torus, checking all configurations and determining global bifurcations. LeBlanc and Langford [38] used for the same Hopf bifurcation Lyapunov–Schmidt theory and singularity theory to study only these 1-dimensional tori. Luongo et al. [40] applied a multiple timescale analysis to the resonant 1:2 and 1:3 double Hopf bifurcation in a straightforward perturbative approach. They perform an extensive numerical analysis, finding several instances of resonance droplets. Volkov [52] takes $n \geq 2$ and studies the persistence of n-dimensional quasi-periodic tori at a 1:2 double Hopf normal resonance. Finally, Revel et al. [44–46] study 1:2 and 2:3 resonant double Hopf bifurcations numerically.

Remarks.

- Already in the work of Guckenheimer and Holmes [27] on the non-resonant case the treatment was divided into 12 cases. In this paper we focus on the case labelled VIa in [27], where a subordinate Hopf bifurcation takes place after reduction of the $\mathbb{T}^n \times \mathbb{T}^2$ symmetry. Next to this exemplary case we note that our approach also applies to all other cases as treated by Knobloch and Proctor [32].
- Next to the subordinate bifurcations of co-dimension 1 we also meet bifurcations of co-dimension 2 that act as organising centres of the dynamics. These are subordinate resonant Hopf bifurcations, fold-Hopf bifurcations, and blue sky bifurcations. Also compare with [5,12,48,50,53]. The fold-Hopf bifurcation does not seem to have been noticed earlier in the literature and a full treatment is outside the present scope, so we refer to [9].

- In the sequel we introduce the invariants τ_j, $j = 1, 2, 3, 4$. Here τ_1 and τ_2 generate the $\mathbb{T}^2$-symmetry, while τ_3 and τ_4 are a global version of the resonant angle. This systematic approach is standard for Hamiltonian systems, and has already been used in [32] for the 1:2 resonance. We shall encounter 3-dimensional versions of the Arnol'd resonance tongues as met in families of circle diffeomorphisms. The intersection with a transverse plane has the form of a droplet, see Figs. 5 and 6.

1.3. Outline

Our contribution is to establish the geometry of the resonance droplet – the present higher dimensional version of the resonance gap – in a generic three-parameter unfolding of a general $\ell_1{:}\ell_2$ resonant double Hopf bifurcation. We exclude only the strongly resonant 1:1 situation. Since we work with n-dimensional tori undergoing a double Hopf bifurcation, all subordinate Hopf bifurcations are put on an equal footing. We leave the occurring quasi-periodic fold-Hopf and heteroclinic bifurcations to future research.

To sketch our results we already refer to the bifurcation diagram in Fig. 2, which describes the truncated normal form after reduction of a $\mathbb{T}^n \times \mathbb{T}^2$ symmetry. From this the symmetric skeleton is reconstructed. The final step is to use perturbation theory back to the original system. This involves both normal hyperbolicity and KAM theory.

2. Linear dynamics

Consider on the phase space $\mathbb{R}^4$ the system

$$\dot{z} \;=\; \Omega(\mu) z. \tag{6}$$

This is the normal part of the normal linear dynamics at the invariant n-torus $\mathbb{T}^n \times \{0\}$.

We assume that the 4 eigenvalues of $\Omega(\mu)$ are of the form $\beta_j(\mu) \pm \mathrm{i}\alpha_j(\mu)$ and that they satisfy $\beta_j(0) = 0$ and $\alpha_j(0) > 0$, for $j = 1, 2$. Analogously to the internal frequency vector $\omega(\mu)$, the normal frequency vector of the invariant torus $\mathbb{T}^n \times \{0\}$ is $\alpha(\mu) = (\alpha_1(\mu), \alpha_2(\mu))$. Moreover, we assume that the normal frequencies are in normal–normal resonance, see (5). If necessary after rescaling time, it can be achieved that $\alpha_1(0)$ takes some given value, for instance $\alpha_1(0) = \ell_1$ which then implies $\alpha_2(0) = \ell_2$. Finally, we can assume that $\gcd(\ell_1, \ell_2) = 1$. Normal–normal resonances at Hopf bifurcation may occur generically in families depending on three or more parameters.

Introducing complex variables $Z_j = z_{2j-1} + \mathrm{i} z_{2j}$, $j = 1, 2$, at $\mu = 0$ the system (6) takes the form

$$\dot{Z}_j \;=\; \mathrm{i}\alpha_j(0) Z_j.$$

Under the linear flow there are four basic invariants

$$\tau_1 \;=\; \tfrac{1}{2} Z_1 \bar{Z}_1, \quad \tau_3 \;=\; \frac{\operatorname{Re} Z_1^{\ell_2} \bar{Z}_2^{\ell_1}}{\ell_1! \ell_2!}, \tag{7a}$$

$$\tau_2 \;=\; \tfrac{1}{2} Z_2 \bar{Z}_2, \quad \tau_4 \;=\; \frac{\operatorname{Im} Z_1^{\ell_2} \bar{Z}_2^{\ell_1}}{\ell_1! \ell_2!}, \tag{7b}$$

i.e. all other functions that are invariant under the flow of (6) can be expressed as functions of the τ_k. These invariants are related by the syzygy

$$\tau_1^{\ell_2} \tau_2^{\ell_1} \;-\; G_\ell (\tau_3^2 + \tau_4^2) \;=\; 0, \quad G_\ell \;=\; \frac{(\ell_1!)^2 (\ell_2!)^2}{2^{\ell_1 + \ell_2}}.$$

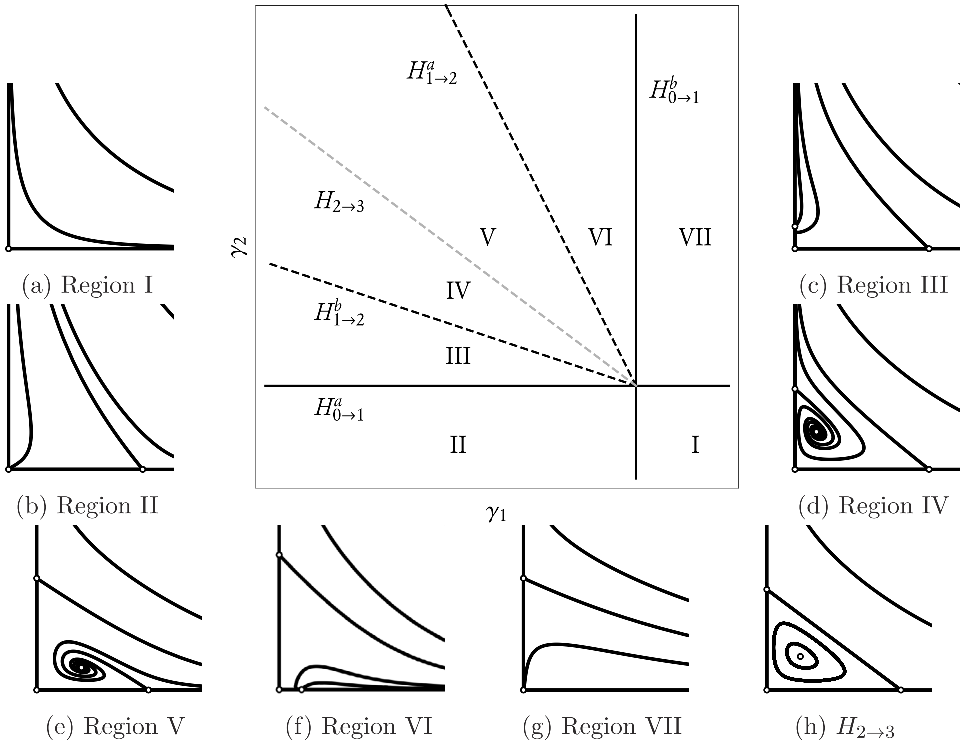

Fig. 2. Bifurcation diagram of (17) with $P = \left(\begin{smallmatrix} 2 & -1 & 3 \\ -1 & -1 & \end{smallmatrix}\right)$. The parameters γ_1 and γ_2 are scaled versions of the real parts β_j of the two pairs of eigenvalues. The regions I–VII in the central picture refer to the surrounding phase portraits on the basis $\mathscr{B}$. See the main text for the coding of the subordinate Hopf bifurcations.

The first two invariants are related to polar co-ordinates by the formula $Z_j = \sqrt{2\tau_j}\mathrm{e}^{\mathrm{i}\phi_j}$. At $\mu = 0$ the angles ϕ_j have the equations of motion

$$\dot{\phi}_j = \alpha_j(0), \quad j = 1, 2.$$

As the frequencies are in resonance, the orbits foliate each $\mathbb{T}^2$ into closed 1-dimensional orbits. This is brought out explicitly by introducing resonance-adapted angles (θ, ϑ) such that

$$\theta = \ell_2\phi_1 - \ell_1\phi_2, \tag{8a}$$

$$\vartheta = m_1\phi_1 + m_2\phi_2. \tag{8b}$$

The right hand side of (8b) is the inner product $\langle m \mid \phi\rangle$. We define $\ell^\perp := (\ell_2, -\ell_1)$ to write the right hand side of (8a) as $\langle \ell^\perp \mid \phi\rangle$

In order that Eqs. (8) determine a torus diffeomorphism, the m_j have to be chosen such that the matrix $\left(\begin{smallmatrix} \ell_2 & -\ell_1 \\ m_1 & m_2 \end{smallmatrix}\right)$ is unimodular. This is possible as $\gcd(\ell_1, \ell_2) = 1$. The invariants τ_3 and τ_4 relate to the resonance-adapted angles by

$$\tau_3 = \sqrt{G_\ell \tau_1^{\ell_2}\tau_2^{\ell_1}}\cos\theta \quad \text{and} \quad \tau_4 = \sqrt{G_\ell \tau_1^{\ell_2}\tau_2^{\ell_1}}\sin\theta\,. \tag{9}$$

In these variables, the linear dynamics is given by

$$\begin{aligned} \dot{\tau}_j &= 0, \quad j = 1, \ldots, 4, \\ \dot{\theta} &= 0, \quad \text{(redundant)}, \\ \dot{\vartheta} &= m_1\alpha_1(0) + m_2\alpha_2(0) = 1, \end{aligned} \tag{10}$$

making ϑ a 'fast' angle. In appropriate co-ordinates the linear family $\dot{z} = \Omega(\mu)z$ is given by

$$\Omega(\mu) = \begin{pmatrix} \beta_1(\mu) & -\alpha_1(\mu) & 0 & 0 \\ \alpha_1(\mu) & \beta_1(\mu) & 0 & 0 \\ 0 & 0 & \beta_2(\mu) & -\alpha_2(\mu) \\ 0 & 0 & \alpha_2(\mu) & \beta_2(\mu) \end{pmatrix}.$$

In terms of the complex variables this simplifies, first to

$$\dot{Z}_j = (\beta_j(\mu) + \mathrm{i}\alpha_j(\mu))Z_j, \quad j = 1, 2,$$

and then to

$$\dot{Z}_j = (\mathrm{i}\alpha_j(0) + \beta_j + \mathrm{i}\delta_j)Z_j,$$

where the $\delta_j = \alpha_j(\mu) - \alpha_j(0)$ detune the normal frequencies and form, together with $\beta_j = \beta_j(\mu)$, $j = 1, 2$, the new independent parameters. In fact, we have passed to $\mu = (\delta_1, \delta_2, \beta_1, \beta_2, \nu)$, where $\nu \in \mathbb{R}^{s-4}$ is a mute parameter. According to [1] this is a versal unfolding.

3. Normal form

We now add the higher order terms to the normal linear system. On the phase space $\mathbb{T}^n \times \mathbb{R}^4$ the system becomes

$$\begin{aligned} \dot{x} &= f(x, z, \mu) = \omega(\mu) + \tilde{f}(x, z, \mu), \\ \dot{z} &= h(x, z, \mu) = \Omega(\mu)z + \tilde{h}(x, z, \mu), \end{aligned}$$

where $\tilde{f} = O(|z|)$ and $\tilde{h} = O(|z|^2)$. To this system are associated the vector field

$$X = f\partial_x + h\partial_z \tag{11}$$

and its normal linear part $L = \omega\partial_z + \Omega z\partial_z$. From the previous section we retain the assumptions on the eigenvalues of $\Omega(\mu)$ and the complex variables Z_j. In these terms, the system takes the form

$$\begin{aligned} \dot{x} &= f(x, Z, \bar{Z}, \mu) = \omega(\mu) + \tilde{f}(x, Z, \bar{Z}, \mu), \\ \dot{Z}_1 &= h_1(x, Z, \bar{Z}, \mu) = (\mathrm{i}\alpha_1(0) + \beta_1 + \mathrm{i}\delta_1)Z_1 + \tilde{h}_1(x, Z, \bar{Z}, \mu), \\ \dot{Z}_2 &= h_2(x, Z, \bar{Z}, \mu) = (\mathrm{i}\alpha_2(0) + \beta_2 + \mathrm{i}\delta_2)Z_2 + \tilde{h}_2(x, Z, \bar{Z}, \mu), \end{aligned}$$

where $\mu_1 = \delta_1$, $\mu_2 = \delta_2$, $\mu_3 = \beta_1$ and $\mu_4 = \beta_2$, while the mute parameter ν has been dropped. Let us define $|k| = |k_1| + |k_2| + \cdots + |k_n|$.

Theorem 3.1 (*Normal Form*)**.** *Let $\ell \in \mathbb{Z}^2$ be such that $0 < \ell_1 < \ell_2$. Consider the real analytic vector field (11) where for $\kappa > n - 1$ and $\Gamma > 0$ the frequency vector (ω, α) at $\mu = 0$ satisfies the Diophantine conditions*

$$\left|\langle k' \mid \omega(0)\rangle + \langle \ell' \mid \alpha(0)\rangle\right| \geq \frac{\Gamma}{(|k'| + |\ell'|)^\kappa} \tag{12}$$

for all $(k', \ell') \in \mathbb{Z}^n \times \mathbb{Z}^2$, *excepting* $(k', \ell') = (0, \ell^\perp)$ *and its integer multiples. For given order* $M \in \mathbb{N}$ *of normalisation there is a diffeomorphism*

$$\Phi \; : \; \mathbb{T}^n \times \mathbb{C}^2 \times \mathbb{R}^s \longrightarrow \mathbb{T}^n \times \mathbb{C}^2 \times \mathbb{R}^s,$$

real analytic in x, Z, $\bar{Z}$ *and* μ, *close to the identity at* $(Z, \mu) = (0, 0)$, *such that the following holds.*
The vector field X *is transformed into normal form*

$$\Phi_* X \;=\; N \;+\; R. \tag{13}$$

The lower order part N *is*

$$\begin{aligned} N \;=\;& \omega(0)\partial_x \;+\; (\mathrm{i}\alpha_1(0) + \beta_1 + \mathrm{i}\delta_1) Z_1 \partial_{Z_1} \;+\; (\mathrm{i}\alpha_2(0) + \beta_2 + \mathrm{i}\delta_2) Z_2 \partial_{Z_2} \\ &+ \sum_m C_m^0 \prod_{j=1}^4 \tau_j^{m_j} \prod_{k=1}^s \mu_k^{m_{4+k}} \partial_x \\ &+ \sum_m C_m^1 \prod_{j=1}^4 \tau_j^{m_j} \prod_{k=1}^s \mu_k^{m_{4+k}} Z_1 \partial_{Z_1} \\ &+ \sum_m C_m^2 \prod_{j=1}^4 \tau_j^{m_j} \prod_{k=1}^s \mu_k^{m_{4+k}} Z_2 \partial_{Z_2} \\ &+ \; c.c., \end{aligned}$$

where c.c. is short for complex conjugate, $C_m^j \in \mathbb{C}$ *and* $m \in \mathbb{N}^{4+s}$ *with*

$$2 \;\leq\; 2(m_1 + m_2) \;+\; |\ell|(m_3 + m_4) \;+\; \sum_{j=1}^s m_{4+j} \;\leq\; M.$$

The remainder R *satisfies the estimate*

$$R \;=\; O_{M+1}(|Z|, |\mu|)\partial_x \;+\; O_{M+1}(|Z|, |\mu) Z_1 \partial_{Z_1} \;+\; O_{M+1}(|Z|, |\mu) Z_2 \partial_{Z_2}.$$

The proof relies on a succession of normal form transformations, see e.g. [9]. Note that in the present notation the part $h_{\mathrm{N}}\partial_z$ of (1) enters N and the part $h_{\mathrm{R}}\partial_z$ of (1) enters R.

To study the resonance, we take the truncation order $M = \max(4, |\ell|)$ such that the lower order part N only contains terms constant and linear in τ_3 and τ_4. It can then be written in the form

$$\begin{aligned} \dot{x} \;&=\; \omega(\mu) \;+\; \hat{f}(\tau_1, \tau_2, \mu) \;+\; a_0(\mu)\tau_3 \;+\; c_0(\mu)\tau_4, \\ \dot{Z}_j \;&=\; \big(\mathrm{i}\alpha_j(0) \;+\; \beta_j \;+\; \mathrm{i}\delta_j \;+\; p_j(\tau_1, \tau_2, \mu) \;+\; \mathrm{i}q_j(\tau_1, \tau_2, \mu) \\ &\qquad +\; [a_j(\mu) + \mathrm{i}b_j(\mu)]\tau_3 \;+\; [c_j(\mu) + \mathrm{i}d_j(\mu)]\tau_4\big)\, Z_j, \qquad j = 1, 2, \end{aligned}$$

where $\hat{f}(0, 0, \mu) = 0$ and $p_j(0, 0, \mu) = q_j(0, 0, \mu) = 0$.

The form of these equations already suggests that, after discarding the strong 1:1 resonance, there are still three distinct situations.

- The first case is $|\ell| = 3$ – the 1:2 resonance – where the terms τ_3 and τ_4 are larger than the terms τ_1^2 and τ_2^2.
- The second case is $|\ell| = 4$ – the 1:3 resonance – where these terms are of the same order of magnitude.

- The third case is $|\ell| \geq 5$ – higher order resonances – where the terms τ_3 and τ_4 are smaller than the terms τ_1^2 and τ_2^2.

4. Analysis of the truncated normal form

We drop the remainder R from the normal form vector field (13) to obtain the $\mathbb{T}^n \times \mathbb{T}^1$ symmetric normal form truncation N. Reducing the $\mathbb{T}^n$ symmetry we obtain normal dynamics on $\mathbb{R}^4$ that still has a $\mathbb{T}$ symmetry. Abusing notation slightly, we also denote this reduced vector field by N.

Equilibria of the reduced N are usually called relative equilibria. Observe that these correspond to invariant n-tori of the unreduced normal form truncation on $\mathbb{T}^n \times \mathbb{R}^4$. In fact the reduced truncation equals the unreduced truncation if $n = 0$: for this reason the relative equilibria are sometimes referred to as 0-tori.

Similarly periodic orbits of the reduced N, which correspond to invariant $(n + 1)$-tori on $\mathbb{T}^n \times \mathbb{R}^4$, are called relative periodic orbits or 1-tori .

4.1. Passing to invariants

Recall formula (9) that relates τ_3 and τ_4 to τ_1, τ_2 and the resonant angle θ. Compared to polar co-ordinates, the invariants τ_1 and τ_2 take the part of the radii, whereas τ_3 and τ_4 take the part of $\cos\theta$ and $\sin\theta$.

Expressed in invariants, the normal form truncation N reads as

$$\begin{aligned}
\dot\tau_1 &= 2\,(\beta_1 + p_1 + a_1\tau_3 + c_1\tau_4)\,\tau_1,\\
\dot\tau_2 &= 2\,(\beta_2 + p_2 + a_2\tau_3 + c_2\tau_4)\,\tau_2,\\
\dot\tau_3 &= (\ell_2(\beta_1 + p_1 + a_1\tau_3 + c_1\tau_4) + \ell_1(\beta_2 + p_2 + a_2\tau_3 + c_2\tau_4))\,\tau_3\\
&\quad - (\ell_2(\delta_1 + q_1 + b_1\tau_3 + d_1\tau_4) - \ell_1(\delta_2 + q_2 + b_2\tau_3 + d_2\tau_4))\,\tau_4,\\
\dot\tau_4 &= (\ell_2(\delta_1 + q_1 + b_1\tau_3 + d_1\tau_4) - \ell_1(\delta_2 + q_2 + b_2\tau_3 + d_2\tau_4))\,\tau_3\\
&\quad + (\ell_2(\beta_1 + p_1 + a_1\tau_3 + c_1\tau_4) + \ell_1(\beta_2 + p_2 + a_2\tau_3 + c_2\tau_4))\,\tau_4.
\end{aligned}$$

We introduce

$$A = \begin{pmatrix} a_1 & c_1 \\ a_2 & c_2 \end{pmatrix}, \quad B = \begin{pmatrix} b_1 & d_1 \\ b_2 & d_2 \end{pmatrix}.$$

Preparing for a Taylor expansion of the right hand side, we also introduce

$$p_{ij}(\mu) = \frac{\partial p_i}{\partial \tau_j}(0, 0, \mu), \quad P(\mu) = \begin{pmatrix} p_{11}(\mu) & p_{12}(\mu) \\ p_{21}(\mu) & p_{22}(\mu) \end{pmatrix},$$

as well as

$$q_{ij}(\mu) = \frac{\partial q_i}{\partial \tau_j}(0, 0, \mu), \quad Q(\mu) = \begin{pmatrix} q_{11}(\mu) & q_{12}(\mu) \\ q_{21}(\mu) & q_{22}(\mu) \end{pmatrix}.$$

We zoom in on the origin of $\mathbb{R}^4$ by scaling time, the invariants and the parameters as

$$t = \varepsilon^{-2}\tilde t, \quad \tau_j = \varepsilon^2\sigma_j, \quad \tau_{j+2} = \varepsilon^{|\ell|}\psi_j, \quad \beta_j = \varepsilon^2\gamma_j, \quad \delta_j = \varepsilon^2\eta_j, \quad j = 1, 2,$$

thereby splitting τ into the amplitude σ and the phase ψ — recall from (9) that ψ is a scaled version of $\cos\theta$ and $\sin\theta$. This allows to introduce $\tilde p$ and $\tilde q$ by

$$p(\varepsilon^2\sigma, \mu) = \varepsilon^2 P(\mu)\sigma + \varepsilon^4\tilde p(\sigma, \varepsilon^2, \mu),$$

$$q(\varepsilon^2\sigma,\mu) \;=\; \varepsilon^2 Q(\mu)\sigma \;+\; \varepsilon^4\tilde{q}(\sigma,\varepsilon^2,\mu).$$

Finally, the detuning δ of the frequencies now results in the parameter

$$\xi \;=\; \langle \ell^\perp \mid \eta\rangle \;=\; \varepsilon^{-2}\langle \ell^\perp \mid \delta\rangle \tag{14}$$

that detunes the frequency ratio.

Introduce $\ell^* := (\ell_2, \ell_1)$, and, for a vector $y \in \mathbb{R}^\nu$, the $\nu \times \nu$ matrix $\operatorname{diag}(y)$ as the diagonal matrix whose i'th diagonal element is y_i. The equations of motion defined by N can then be written as

$$\dot{\sigma} \;=\; 2\operatorname{diag}(\gamma + P\sigma + \varepsilon^2\tilde{p} + \varepsilon^{|\ell|-2}A\psi)\sigma, \tag{15a}$$

$$\dot{\psi} \;=\; \begin{pmatrix} \langle \ell^* \mid \gamma + P\sigma + \varepsilon^2\tilde{p} + \varepsilon^{|\ell|-2}A\psi\rangle & -\xi - \langle \ell^\perp \mid Q\sigma + \varepsilon^2\tilde{q} + \varepsilon^{|\ell|-2}B\psi\rangle \\ \xi + \langle \ell^\perp \mid Q\sigma + \varepsilon^2\tilde{q} + \varepsilon^{|\ell|-2}B\psi\rangle & \langle \ell^* \mid \gamma + P\sigma + \varepsilon^2\tilde{p} + \varepsilon^{|\ell|-2}A\psi\rangle \end{pmatrix}\psi. \tag{15b}$$

The intricacies of the resonance at hand are encoded in (15b). The syzygy takes the form

$$\sigma_1^{\ell_2}\sigma_2^{\ell_1} \;-\; G_\ell(\psi_1^2+\psi_2^2) \;=\; 0. \tag{16}$$

The equations of motions defined by N are then defined on the reduced phase space

$$\mathscr{P} \;=\; \left\{ (\sigma,\psi) \in \mathbb{R}^2 \times \mathbb{R}^2 \;:\; \sigma_1 \geq 0,\; \sigma_2 \geq 0,\; \psi_1^2+\psi_2^2 \;=\; \frac{\sigma_1^{\ell_2}\sigma_2^{\ell_1}}{G_\ell} \right\},$$

which is a semi-algebraic variety. Geometrically, $\mathscr{P}$ is a degenerate circle bundle over the basis $\mathscr{B} = \mathbb{R}^2_{\geq 0}$ that is degenerate at the boundary of $\mathscr{B}$.

As we are not trying to perform an exhaustive analysis, we restrict the analysis to the situation where there is a subordinate Hopf bifurcation from a 2-dimensional to a 3-dimensional torus. In particular, we investigate the equations of motion (15) under the assumptions that $p_{11} > 0$, $p_{22} < 0$ and $\det P > 0$.

4.2. Equilibria on the basis $\mathscr{B}$

For $\varepsilon = 0$ the system (15) simplifies to

$$\dot{\sigma} \;=\; 2\operatorname{diag}(\gamma + P\sigma)\sigma, \tag{17a}$$

$$\dot{\psi} \;=\; \begin{pmatrix} \langle \ell^* \mid \gamma + P\sigma\rangle & -\xi - \langle \ell^\perp \mid Q\sigma\rangle \\ \xi + \langle \ell^\perp \mid Q\sigma\rangle & \langle \ell^* \mid \gamma + P\sigma\rangle \end{pmatrix}\psi. \tag{17b}$$

Remark that the system (17) is skew: the basis dynamics (17a), which is defined on the basis $\mathscr{B}$ of $\mathscr{P}$, is decoupled from the fibre dynamics (17b) and, in fact, drives the fibre dynamics. Also note that the basis dynamics has Lotka–Volterra structure; that is, the components of the vector field are quadratic polynomials and the axes $\sigma_1 = 0$ and $\sigma_2 = 0$ are invariant. Finally, note that (15a) is the same as in the non-resonant case, compare with [27,34,39].

Equilibria of the basis dynamics are the central equilibrium

$$\bar{\sigma} \;=\; 0,$$

which corresponds to the equilibrium of the original system on $\mathbb{R}^4$, the boundary equilibria

$$\bar{\sigma} \;=\; \begin{pmatrix} -\gamma_1/p_{11} \\ 0 \end{pmatrix}, \quad \bar{\sigma} \;=\; \begin{pmatrix} 0 \\ -\gamma_2/p_{22} \end{pmatrix},$$

which correspond to periodic orbits in the original system, and the interior equilibrium

$$\bar{\sigma} \;=\; -P^{-1}\gamma,$$

which corresponds to an invariant 2-torus. All equilibria are defined for those values of γ such that $\bar{\sigma}_1 \geq 0$ and $\bar{\sigma}_2 \geq 0$.

4.3. Hopf bifurcations on the basis $\mathscr{B}$

Linearising the flow to investigate the stability of the equilibria yields

$$\dot{\sigma} \;=\; \begin{pmatrix} \gamma_1 + 2p_{11}\bar{\sigma}_1 + p_{12}\bar{\sigma}_2 & p_{12}\bar{\sigma}_1 \\ p_{21}\bar{\sigma}_2 & \gamma_2 + p_{21}\bar{\sigma}_1 + 2p_{22}\bar{\sigma}_2 \end{pmatrix} (\sigma - \bar{\sigma}) \;+\; O(\|\sigma - \bar{\sigma}\|^2).$$

For the central equilibrium, this reduces to

$$\dot{\sigma} \;=\; \begin{pmatrix} \gamma_1 & 0 \\ 0 & \gamma_2 \end{pmatrix} \sigma \;+\; O(\|\sigma\|^2).$$

The central equilibrium is attracting if $\gamma_j < 0$ for $j = 1, 2$ and repelling if $\gamma_j > 0$ for $j = 1, 2$. Correspondingly, the curves

$$H^a_{0\to 1} \;:\; \gamma_1 \;=\; 0 \qquad \text{and} \qquad H^b_{0\to 1} \;:\; \gamma_2 \;=\; 0$$

are Hopf bifurcation curves for the original system, where a 0-torus changes stability.

The 1-tori in $\mathbb{R}^4$ bifurcating off from the origin correspond to the boundary equilibria. These tori pass in turn through a secondary Hopf bifurcation. For the boundary equilibrium $\bar{\sigma} = (-\gamma_1/p_{11}, 0)$, which under our assumptions on P exists if $\gamma_1 < 0$, we obtain

$$\dot{\sigma} \;=\; \begin{pmatrix} -\gamma_1 & -\frac{p_{21}}{p_{11}}\gamma_1 \\ 0 & \gamma_2 - \frac{p_{21}}{p_{11}}\gamma_1 \end{pmatrix} (\sigma - \bar{\sigma}) \;+\; O(\|\sigma - \bar{\sigma}\|^2).$$

Hence, this equilibrium changes from attractor to saddle at

$$H^a_{1\to 2} \;:\; p_{21}\gamma_1 \;-\; p_{11}\gamma_2 \;=\; 0.$$

Similarly, the boundary equilibrium $\bar{\sigma} = (0, -\gamma_2/p_{22})$ changes from attractor to saddle at

$$H^b_{1\to 2} \;:\; p_{22}\gamma_1 \;-\; p_{12}\gamma_2 \;=\; 0.$$

Linearising the flow at the interior equilibrium yields

$$\dot{\sigma} \;=\; \begin{pmatrix} p_{11}\bar{\sigma}_1 & p_{12}\bar{\sigma}_1 \\ p_{21}\bar{\sigma}_2 & p_{22}\bar{\sigma}_2 \end{pmatrix} (\sigma - \bar{\sigma}) \;+\; O(\|\sigma - \bar{\sigma}\|^2).$$

The characteristic equation of the matrix on the right hand side is

$$0 \;=\; \det \begin{pmatrix} p_{11}\bar{\sigma}_1 - \lambda & p_{12}\bar{\sigma}_1 \\ p_{21}\bar{\sigma}_2 & p_{22}\bar{\sigma}_2 - \lambda \end{pmatrix} \;=\; \bar{\sigma}_1\bar{\sigma}_2 \det \begin{pmatrix} p_{11} - \lambda/\bar{\sigma}_1 & p_{12} \\ p_{21}\bar{\sigma}_2 & p_{22} - \lambda/\bar{\sigma}_2 \end{pmatrix} .$$

The equilibrium has imaginary eigenvalues if

$$\operatorname{trace} \begin{pmatrix} p_{11}\bar{\sigma}_1 & p_{12}\bar{\sigma}_1 \\ p_{21}\bar{\sigma}_2 & p_{22}\bar{\sigma}_2 \end{pmatrix} \;=\; p_{11}\bar{\sigma}_1 + p_{22}\bar{\sigma}_2 \;=\; 0$$

and

$$\det \begin{pmatrix} p_{11}\bar{\sigma}_1 & p_{12}\bar{\sigma}_1 \\ p_{21}\bar{\sigma}_2 & p_{22}\bar{\sigma}_2 \end{pmatrix} \;=\; (\det P)\bar{\sigma}_1\bar{\sigma}_2 \;>\; 0.$$

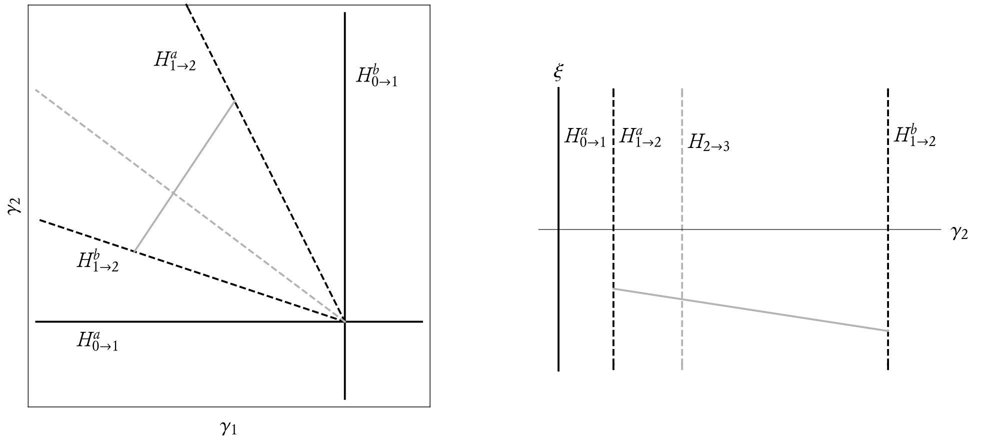

Fig. 3. The normal form (17) does not fully resolve the resonance droplet, which is shown as a grey segment. In the left hand picture we use the scaled eigenvalue parameters γ_1 and γ_2. In the right hand picture we replace γ_1 by the frequency ξ, defined in (14). Also not resolved is the Hopf line $H_{2\to 3}$, also shown in grey, which should yield a whole range of parameters with periodic orbits on the basis $\mathscr{B}$.

The first condition can only be satisfied if the signs of p_{11} and p_{22} are opposite, as we have assumed. The second condition is always satisfied given our assumption that $\det P > 0$. The first condition can be written as

$$H_{2\to 3} \quad : \quad p_{22}(p_{21} - p_{11})\gamma_1 \; + \; p_{11}(p_{12} - p_{22})\gamma_2 \;=\; 0.$$

It is well-known [27] that this Hopf bifurcation is degenerate, and that the base system has a first integral at the $H_{2\to 3}$ bifurcation value. Using the condition, the normal frequency at Hopf bifurcation can be expressed as a function of the scaled parameter γ_1 as

$$\sqrt{(\det P)\bar{\sigma}_1\bar{\sigma}_2} \;=\; |\gamma_1||p_{21} - p_{11}|\sqrt{(p_{12}p_{21} - p_{11}p_{22})p_{11}/p_{22}}.$$

The locations of the Hopf bifurcation curves are illustrated in Fig. 2.

4.4. *Dynamics on the reduced phase space* $\mathscr{P}$

Joining the fibre dynamics (17b) to the basis dynamics (17a), for $\varepsilon = 0$ we find two degeneracies. First, for parameters at the $H_{2\to 3}$ Hopf bifurcation value, the basis dynamics has a first integral. Second, an equilibrium $\bar{\sigma}$ of the basis dynamics corresponds to a limit cycle as long as the frequency $\xi + \langle \ell^\perp \mid Q\bar{\sigma}\rangle$ does not vanish and to a circle of equilibria where it does vanish. In the latter case we speak of a resonance droplet.

Now consider (15) for $\varepsilon > 0$. There are two situations, according to whether the frequency $\xi + \langle \ell^\perp \mid Q\bar{\sigma}\rangle$ of the fibre dynamics does or does not vanish. If $\bar{\sigma}$ is a hyperbolic equilibrium of the basis dynamics and if $\xi + \langle \ell^\perp \mid Q\bar{\sigma}\rangle$ does not vanish, the limit cycle $\{\bar{\sigma}\} \times \mathbb{T}$ survives a small perturbation. If $\bar{\sigma}$ is at the subordinate Hopf bifurcation $H_{2\to 3}$ we have to normalise to higher order than 4 to resolve the degeneracy. As shown in [27] already one additional order suffices. This has consequences only for the low order 1:2 and 1:3 resonances where indeed $|\ell| \leq 4$. For the higher order resonances we already do normalise to order $|\ell| \geq 5$. Note that next to the Hopf line $H_{2\to 3}$ also the resonance bubbles are not fully resolved, see Fig. 3.

In this way the family of periodic orbits at a single parameter value gets re-distributed over a range of parameters, starting at the Hopf bifurcation $H_{2\to 3}$ and ending at the parameter value *Het* of a heteroclinic bifurcation where a closed orbit disappears in a blue sky bifurcation.

4.5. Saddle–node bifurcations on the reduced phase space $\mathscr{P}$

We proceed to find the equilibria of (15), which satisfy the equations

$$0 = \gamma + P\sigma + \varepsilon^2\tilde{p} + \varepsilon^{|\ell|-2}A\psi, \tag{18a}$$
$$0 = \xi + \langle \ell^\perp \mid Q\sigma + \varepsilon^2\tilde{q} + \varepsilon^{|\ell|-2}B\psi\rangle, \tag{18b}$$

together with the syzygy (16).

As P is invertible, which is the only situation we consider, Eq. (18a) can be solved in the form

$$\sigma = \Phi_0(\gamma,\varepsilon^2) + \varepsilon^{|\ell|-2}\Phi_1(\gamma,\varepsilon^2,\varepsilon^{|\ell|-2}A\psi)A\psi$$

where $\Phi_0(\gamma,0) = -P^{-1}\gamma$ and $\Phi_1(\gamma,0,0) = -P^{-1}$. Substitution into (18b) yields

$$0 = \xi + \langle \ell^\perp \mid Q\Phi_0 + \varepsilon^2\tilde{q}\rangle + \varepsilon^{|\ell|-2}\langle \ell^\perp \mid (B+\Phi_1 A)\psi\rangle. \tag{19}$$

To describe the saddle–node bifurcation curves, we perform a blow-up by introducing the scaled parameter ζ as

$$\varepsilon^{|\ell|-2}\zeta = \xi + \langle \ell^\perp \mid Q\Phi_0 + \varepsilon^2\tilde{q}\rangle.$$

Dividing by $\varepsilon^{|\ell|-2}$, this transforms (19) into

$$0 = \zeta + \langle \ell^\perp \mid (B+\Phi_1 A)\psi\rangle. \tag{20}$$

As an equation in ψ, (20) describes a family of curves that for $\varepsilon = 0$ reduces to a family of lines, since Φ_1, A and B are independent of ψ. For fixed values of σ, the syzygy (16) defines a circle. The curves (20) intersect the circle in either zero or two points, or they touch the circle. In the latter situation, we have a saddle–node bifurcation of equilibria, defining the boundaries of a resonance droplet of width $\varepsilon^{|\ell|-2}$. The resulting bifurcation diagram is given in Fig. 4 .

Writing $R^2 = \bar{\sigma}_1^{\ell_2}\bar{\sigma}_2^{\ell_1}/G_\ell$ and $m = (B-PA)^T\ell^\perp$, the condition that the line $\langle m \mid \psi\rangle + \zeta = 0$ touches the circle $|\psi| = R$ implies that $\psi = \alpha m$ for a real scalar α that satisfies $|\alpha| = R/|m|$. For $\varepsilon = 0$ the saddle–node bifurcation condition can then be written as

$$\zeta = \pm|m|R = \pm C\bar{\sigma}_1^{\ell_2/2}\bar{\sigma}_2^{\ell_1/2}. \tag{21}$$

Since a line is flat and a circle has constant curvature, it is clear that – for sufficiently small $\varepsilon > 0$ – the saddle–node bifurcation is nondegenerate.

Eq. (21) shows that the saddle–node curves are the boundaries of a resonance droplet with width proportional to $\bar{\sigma}_1^{\ell_2/2}$ close to the Hopf curve $\bar{\sigma}_1 = 0$ and width proportional to $\bar{\sigma}_2^{\ell_1/2}$ close to the Hopf curve $\bar{\sigma}_2 = 0$. This is illustrated in Figs. 5 and 6.

4.6. Putting it all together

When the saddle–node bifurcation on the invariant circle coincides with the occurrence of two unit Floquet multipliers of the limit circle, we expect a fold-Hopf bifurcation to occur. In Figs. 5 and 6 these are the two points where the line $H_{2\to 3}$ – which ceases to exist inside the resonance droplet – meets the resonance droplet at the boundary.

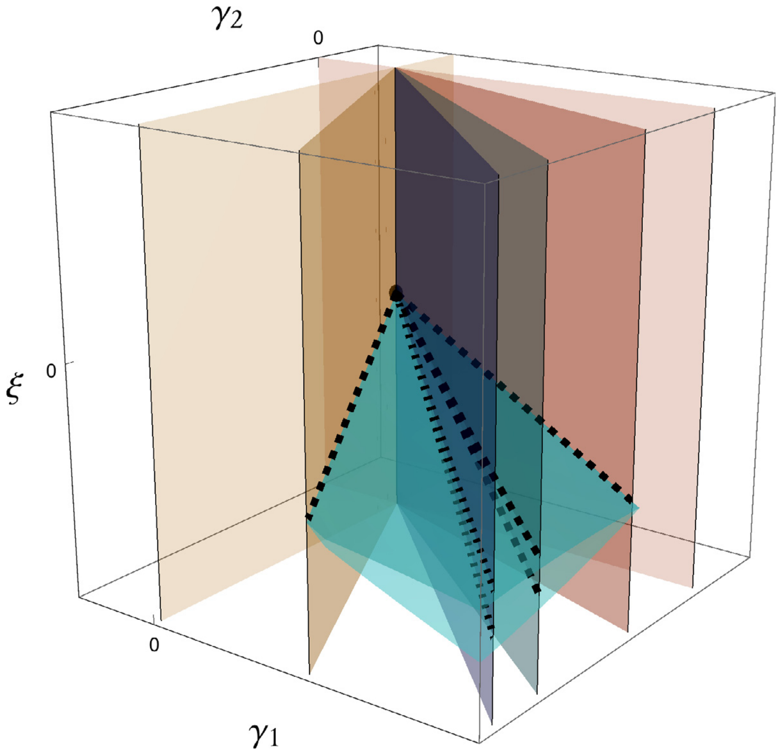

Fig. 4. Local bifurcation diagram of the family (15) in the space of the scaled eigenvalue parameters γ_1, γ_2 and the frequency ξ, defined in (14). The orange planes are the Hopf bifurcations taken over from Fig. 2. In green we furthermore include the saddle–node bifurcations originating from the resonance droplets in Fig. 3. Finally, the purple plane denotes the heteroclinic bifurcations, which originate from resolving the $H_{2\to 3}$ bifurcation. (For interpretation of the references to colour in this figure legend, the reader is referred to the web version of this article.)

5. Dynamics of the full system

In the previous section we analysed the dynamics of the truncated normal form on $\mathbb{R}^4$, i.e. after reduction of the $\mathbb{T}^n$ symmetry. Reconstructing the dynamics of the truncated normal form on $\mathbb{T}^n \times \mathbb{R}^4$ amounts to restoring the driving

$$\dot{x} \;=\; \omega(\mu) \;+\; \hat{f}(\tau_1, \tau_2, \mu) \;+\; a_0(\mu)\tau_3 \;+\; c_0(\mu)\tau_4,$$

which for $\tau = 0$ is conditionally periodic with frequency vector $\omega(\mu)$. On $\mathbb{R}^4$ we still have a $\mathbb{T}$ symmetry in the resonant case and a $\mathbb{T}^2$ symmetry in the non-resonant case, and even in the resonant case if we choose an order of truncation lower than the order $|\ell|$ of τ_3 and τ_4. Reducing the former symmetry takes us to the reduced phase space $\mathscr{P}$; reducing the latter takes us to the basis $\mathscr{B}$ of the circle bundle $\mathscr{P}$.

For the relevant KAM theory, see [10,14,18,22,42,54,55]. The general philosophy is that we first are given a generic integrable (i.e. torus symmetric) system, where the dimension of the torus equals n, $n + 1$ or $n + 2$. The Diophantine conditions (12) determine a ‘Cantorised’ sub-bundle which is nowhere dense, but of large Lebesgue measure for small values of the gap

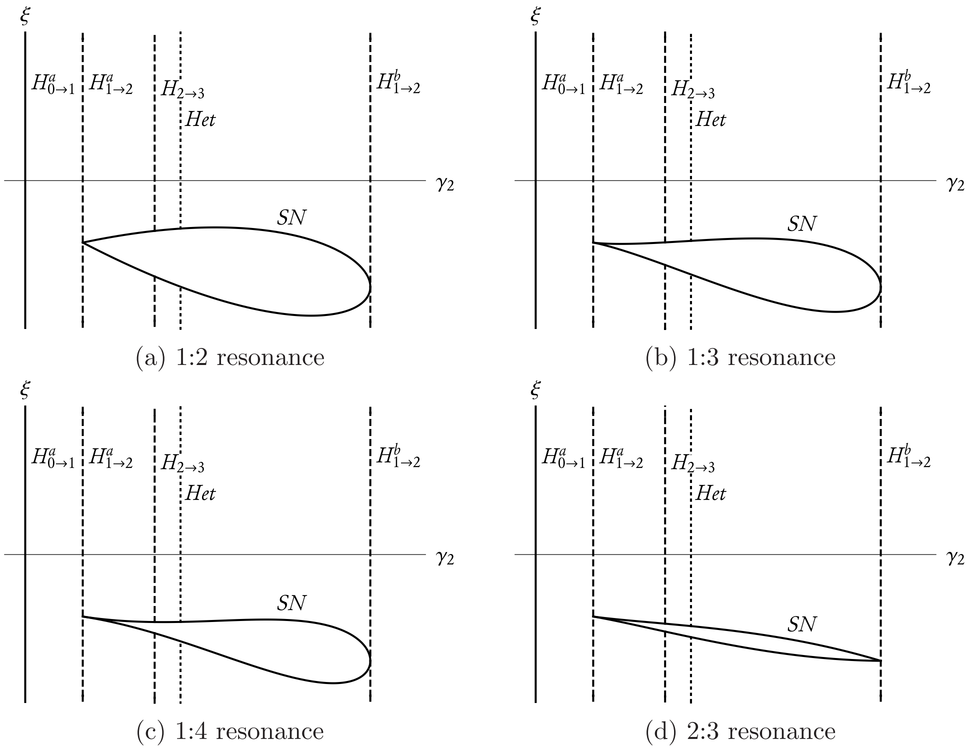

Fig. 5. Vertical sections of the bifurcation diagram given in Fig. 4. So we fix γ_1 and only consider the parameters γ_2 and ξ. Shape of the resonance droplets for the 1:2, the 1:3, the 1:4 and the 2:3 resonance.

parameter Γ. Restricted to this set a Whitney smooth conjugation exists with a subset of the perturbed system. This result is called *quasi-periodic stability*: structural stability restricted to a bundle of Diophantine quasi-periodic tori. The main question here is what happens in the gaps of this Cantorised bundle. In the present dissipative context hyperbolicity plays an important role in the perturbation analysis.

5.1. No resonance

The truncated normal form is not only independent of x but also independent of τ_3 and τ_4 if there is no resonance (5) with $\ell \neq 0$ between the normal frequencies $\alpha_1(0)$ and $\alpha_2(0)$, or if we chose an order of truncation that is lower than the order $|\ell|$ of τ_3 and τ_4 in case there is a resonance $\ell \neq 0$ of the form (5). Reconstructing the dynamics on $\mathbb{R}^4$ from the reduced dynamics on $\mathscr{B}$ is already implicit in Fig. 2. Indeed, it is the reconstructed toral dynamics that turns the pitchfork bifurcations that are actually visible in that figure into the Hopf bifurcations $H^{a,b}_{0\to1}$ and $H^{a,b}_{1\to2}$. On $\mathbb{T}^n \times \mathbb{R}^4$ these then reconstruct to Hopf bifurcations of n-tori and $(n+1)$-tori, respectively, resulting in tori of dimensions $n+1$ and $n+2$.

For $n = 0$ persistence of the latter – when perturbing from the normal form back to the original system – has been proved in [39], as has been persistence of the 3-tori resulting from the quasi-periodic Hopf bifurcation $H_{2\to3}$. Persistence of the three types of Hopf bifurcations

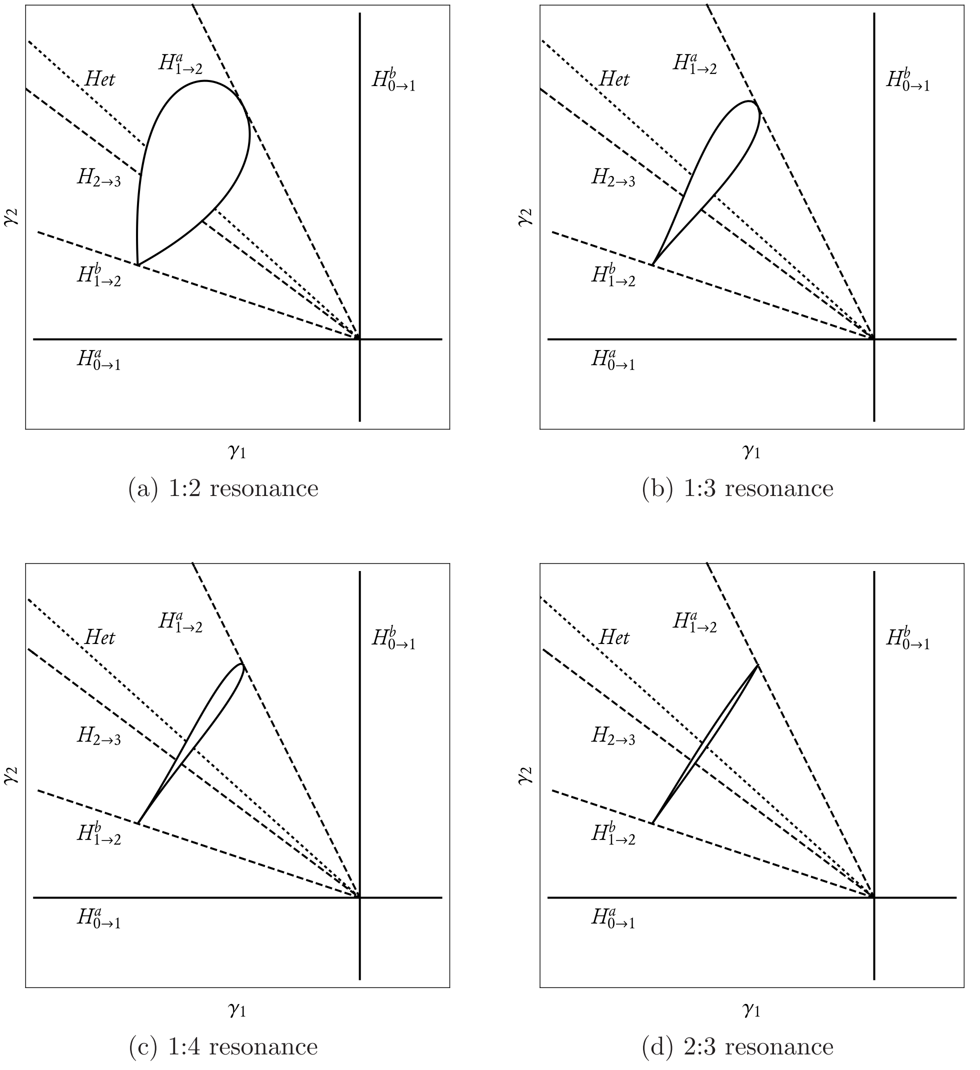

Fig. 6. Horizontal sections of the bifurcation diagram given in Fig. 4. So we fix ξ and only consider the parameters γ_1 and γ_2. Shape of the resonance droplets for the 1:2, the 1:3, the 1:4 and the 2:3 resonance.

of n-tori, $(n+1)$-tori and $(n+2)$-tori follows from [3,22], see also [9]. We remark that the specialised approach in [39] yields the same order $\varepsilon^{1/18}$ as the general treatment in [3]. Indeed, in [3] we have a general normal form as in Theorem 3.1, where we have to go up to 8th order. Accounting for each normalisation step by ε^2, the remainder terms turn out to be of order ε^{18}.

The gaps left open when Cantorising the attracting tori to prove persistence using KAM theory can be closed using normal hyperbolicity to obtain invariant tori on which the flow is no longer quasi-periodic, see Fig. 7; also compare with [8] and results cited therein. There seem to be no claims concerning the subordinate heteroclinic bifurcation in the literature.

5.2. *Higher order resonances*

Here we normalise op to order $|\ell| \geq 5$. This makes the 1:4 and 2:3 resonances still special among the higher order resonances as normalising up to 5th order to resolve the Hopf bifurcation $H_{2\to3}$ automatically includes τ_3 and τ_4 into the normal form. Note that the opening of the resonance bubbles is dictated by ℓ_1 and ℓ_2 separately, see e.g. Figs. 5c and 6c.

Where the line $H_{2\to3}$ meets the resonance bubble we have a fold-Hopf bifurcation; in fact the line ceases to exist inside the resonance bubble. Next to the Hopf bifurcations $H^{a,b}_{0\to1}$ of n-tori, for the persistence of which we again refer to [3,9,22,39], this leaves us with six special points: the two Hopf bifurcations $H^{a,b}_{1\to2}$ of $(n+1)$-tori with a normal-internal resonance, the two fold-Hopf bifurcations and the two heteroclinic bifurcations at the boundary of the resonance bubble (which we do not further comment upon).

5.3. *The* 1:3 *resonance*

In this case $|\ell| - 2 = 2$, which means that we have two competing influences in the normal form. Hence, the relative strengths of the coefficients $\tilde{p}$ and $A\psi$ in (15) decide whether we have dynamics similar to the previous subsection or dynamics similar to the following subsection.

5.4. *The* 1:2 *resonance*

Although the invariants τ_3 and τ_4 have order $|\ell| = 3$ in this case, we still work with a 5th order normal form to resolve the Hopf bifurcation $H_{2\to3}$. In this way not only the linear terms τ_3 and τ_4 enter the normal form, but also the four 5th order terms $\tau_i\tau_j$ with $i = 1, 2$ and $j = 3, 4$. We wonder whether the subordinate fold-Hopf bifurcation requests even higher order terms of the normal form or whether the 5th order terms are already sufficient, again see [9].

At the end points of the resonance bubble we have periodic Hopf bifurcations $H^{a,b}_{1\to2}$ with normal-internal resonances 1:1 and 1:2, respectively.

6. Final remarks

The $\mathbb{T}^1$ or $\mathbb{T}^2$ symmetric normal form analysis forms a kind of skeleton of the total dynamics, which is recovered when adding the non-symmetric higher order terms.

First note that normal forms of any finite order keep the toroidal symmetry. That means that the non-symmetric terms are flat, that is, of infinite order. We expect these terms to be exponentially small in the real analytic context [8,13,17,23,31,41]. In the present dissipative context the higher order resonances in the Diophantine conditions (12) give rise to infinite arrays of ‘small’ resonance bubbles [2–4,8,9,19–21], where the array ‘runs along’ the bifurcation manifolds as given by the quasi-periodic sub-bundle, compare with the discussion at the beginning of Section 5. The paper [8] exactly uses the quasi-periodic Hopf bifurcation as a leading example.

Inside the bubbles the complexity is large both in the dissipative and the conservative context, which is illustrated by the papers [15,16,51].

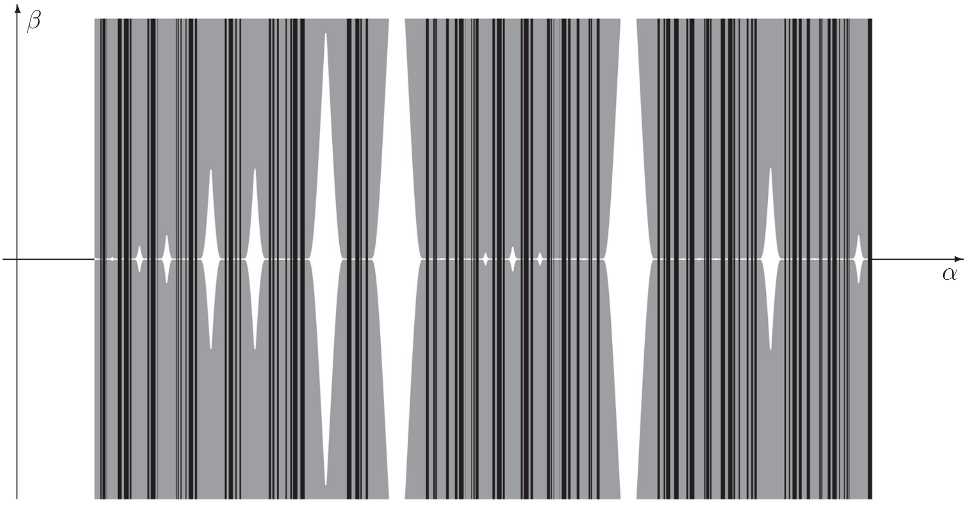

Fig. 7. Parameter sets with persistent invariant tori and the subset of persistent quasi-periodic invariant tori. The latter (black) set is the product of a Cantor set in the α-direction and the real line in the β-direction: it is nowhere dense. The (white) complement of the former set (which includes the resonance set on the β-axis) is a 'set of ignorance'.
Source: From [8].

References

[1] V.I. Arnol'd, On matrices depending on parameters, Russian Math. Surveys 26 (2) (1971) 29–43.
[2] B.L.J. Braaksma, H.W. Broer, On a quasi-periodic Hopf bifurcation, Ann. Inst. Henri Poincaré Anal. Non linéaire 4 (1987) 115–168.
[3] B.L.J. Braaksma, H.W. Broer, G.B. Huitema, Towards a quasi-periodic bifurcation theory, Mem. Amer. Math. Soc. 83 (# 421) (1990) 83–167.
[4] H.W. Broer, Coupled Hopf-bifurcations: Persistent examples of n–quasiperiodicity given by families of 3-jets, Astérisque 286 (2003) 223–229.
[5] H.W. Broer, R. van Dijk, Re. Vitolo, Survey of strong normal-internal $k : l$ resonances in quasi-periodically driven oscillators for $l = 1, 2, 3$, in: G. Gaeta, Ra. Vitolo, S. Walcher (Eds.), Symmetry and Perturbation Theory, Proceedings of the International Conference SPT 2007, World Scientific, 2007, pp. 45–55.
[6] H.W. Broer, H. Hanßmann, J. Hoo, The quasi-periodic Hamiltonian Hopf bifurcation, Nonlinearity 20 (2007) 417–460.
[7] H.W. Broer, H. Hanßmann, À. Jorba, J. Villanueva, F.O.O. Wagener, Normal-internal resonances in quasi-periodically forced oscillators: a conservative approach, Nonlinearity 16 (2003) 1751–1791.
[8] H.W. Broer, H. Hanßmann, F.O.O. Wagener, Persistence properties of normally hyperbolic tori, Regul. Chaotic Dyn. 23 (2018) 212–225.
[9] H.W. Broer, H. Hanßmann, F.O.O. Wagener, Quasi-Periodic Bifurcation Theory, the Geometry of KAM, Springer, in preparation.
[10] H.W. Broer, G.B. Huitema, M.B. Sevryuk, Quasi-periodic motions in families of dynamical systems: order amidst chaos, in: Lecture Notes in Mathematics, vol. 1645, Springer, 1996.
[11] H.W. Broer, G.B. Huitema, F. Takens, Unfoldings of quasi-periodic tori, Mem. Amer. Math. Soc. 83 (# 421) (1990) 1–81.
[12] H.W. Broer, V. Naudot, R. Roussarie, K. Saleh, F.O.O. Wagener, Organising centres in the semi-global analysis of dynamical systems, Int. J. Appl. Math. Stat. 12 (D07) (2007) 7–36.
[13] H.W. Broer, R. Roussarie, Exponential confinement of chaos in the bifurcation set of real analytic diffeomorphisms, in: H.W. Broer, B. Krauskopf, G. Vegter (Eds.), Global Analysis of Dynamical Systems. Festschrift Dedicated to Floris Takens for His 60th Birthday, Inst. of Phys., Bristol, 2001, pp. 167–210.

[14] H.W. Broer, M.B. Sevryuk, KAM Theory: quasi-periodicity in dynamical systems, in: H.W. Broer, B. Hasselblatt, F. Takens (Eds.), Handbook of Dynamical Systems, Vol. 3, North-Holland, 2010.
[15] H.W. Broer, C. Simó, R. Vitolo, The Hopf-saddle-node bifurcation for fixed points of 3D-diffeomorphisms, analysis of a resonance 'bubble', Physica D 237 (2008) 1773–1799.
[16] H.W. Broer, C. Simó, R. Vitolo, The Hopf-saddle-node bifurcation for fixed points of 3D-diffeomorphisms: the Arnol'd resonance web, Bull. Belg. Math. Soc. Simon Stevin 15 (2008) 769–787.
[17] H.W. Broer, F. Takens, Formally symmetric normal forms and genericity, Dyn. Rep. 2 (1989) 36–60.
[18] H.W. Broer, F. Takens, Dynamical Systems and Chaos, in: Epsilon Uitgaven 64 (2009); Applied Mathematical Sciences, vol. 172, Springer, 2011.
[19] A. Chenciner, Bifurcations des points elliptiques-I. Courbes invariantes, Publ. Math. Inst. Hautes Études 61 (1985) 67–127.
[20] A. Chenciner, Bifurcations des points elliptiques-II. Orbites périodiques et ensembles de Cantor invariants, Invent. Math. 80 (1985) 81–106.
[21] A. Chenciner, Bifurcations des points elliptiques-III. Orbites périodiques de petites périodes et élimination résonnante des couples de courbes invariantes, Publ. Math. Inst. Hautes Études 66 (1987) 5–91.
[22] M.C. Ciocci, A. Litvak-Hinenzon, H.W. Broer, Survey on dissipative KAM theory including quasi-periodic bifurcation theory, in: J. Montaldi, T.S. Raţiu (Eds.), Geometric Mechanics and Symmetry: the Peyresq Lectures, Cambridge University Press, 2005, pp. 303–355.
[23] A. Delshams, P. Gutierrez, Effective stability and KAM theory, J. Differential Equations 128 (1996) 415–490.
[24] R. Devaney, An Introduction to Chaotic Dynamical Systems, second ed., Addison-Wesley, Redwood City, 1989.
[25] S.A. van Gils, M. Krupa, W.F. Langford, Hopf bifurcation with non-semisimple 1:1 resonance, Nonlinearity 3 (1990) 825–850.
[26] M. Golubitsky, M. Krupa, Stability computations for nilpotent Hopf bifurcations in coupled cell systems, Int. J. Bifurcation Chaos 17 (2007) 2595–2603.
[27] J. Guckenheimer, P. Holmes, Nonlinear Oscillations, Dynamical Systems, and Bifurcations of Vector Fields, fifth ed., in: Applied Mathematical Sciences, vol. 42, Springer, 1997.
[28] H. Hanßmann, Local and Semi-Local Bifurcations in Hamiltonian Dynamical Systems — Results and Examples, in: Lecture Notes in Mathematics, vol. 1893, Springer, 2007.
[29] M.W. Hirsch, C.C. Pugh, M. Shub, Invariant Manifolds, in: Lecture Notes in Mathematics, vol. 583, Springer, 1977.
[30] E. Hopf, A mathematical example displaying features of turbulence, Commun. Pure Appl. Math. 1 (1948) 303–322.
[31] A. Jorba, J. Villanueva, On the normal behaviour of partially elliptic lower-dimensional tori of Hamiltonian systems, Nonlinearity 10 (1997) 783–822.
[32] E. Knobloch, M.R.E. Proctor, The double Hopf bifurcation with 2:1 resonance, Proc. R. Soc. Lond. A 415 (1988) 61–90.
[33] A.M. Krasnosel'skii, D.I. Rachinskii, K. Schneider, Hopf bifurcations in resonance 2:1, Nonlinear Anal. 52 (2003) 943–960.
[34] Yu. Kuznetsov, Elements of applied bifurcation theory, in: Applied Mathematical Sciences, vol. 112, Springer, 1995.
[35] L.D. Landau, On the problem of turbulence, C. R. Acad. Sci. l'URSS 44 (1944) 311–314.
[36] L.D. Landau, E.M. Lifshitz, Fluid Mechanics, Pergamon Press, Oxford, 1987.
[37] V.G. LeBlanc, On some secondary bifurcations near resonant Hopf-Hopf interactions, Dyn. Contin. Discrete Impuls. Syst. Ser. B Appl. Algorithms 7 (2000) 405–427.
[38] V. LeBlanc, W.F. Langford, Classifications and unfoldings of 1:2 resonant Hopf bifurcation, Arch. Ration. Mech. Anal. 136 (1996) 305–357.
[39] X. Li, On the persistence of quasi-periodic invariant tori for double Hopf bifurcation of vector fields, J. Differential Equations 260 (2016) 7320–7357.
[40] A. Luongo, A. Paolone, A. Di Egidio, Multiple timescales analysis for 1:2 and 1:3 resonant Hopf bifurcations, Nonlinear Dynam. 34 (2003) 269–291.
[41] A. Morbidelli, A. Giorgilli, Superexponential stability of KAM tori, J. Stat. Phys. 78 (1995) 1607–1617.
[42] J.K. Moser, Convergent series expansion for quasi-periodic motions, Math. Ann. 169 (1967) 136–176.
[43] N.S. Namachchivaya, M.M. Doyle, W.F. Langford, N.W. Evans, Normal form for generalized Hopf bifurcation with non-semisimple 1:1 resonance, Z. Angew. Math. Phys. 45 (1994) 312–335.

[44] G. Revel, D.M. Alonso, J.L. Moiola, Interactions between oscillatory modes near a 2:3 resonant Hopf-Hopf bifurcation, Chaos 20 (2010) 043106.

[45] G. Revel, D.M. Alonso, J.L. Moiola, Numerical semi-global analysis of a 1:2 resonant Hopf-Hopf bifurcation, Physica D 247 (2013) 40–53.

[46] G. Revel, D.M. Alonso, J.L. Moiola, A degenerate 2:3 resonant Hopf-Hopf bifurcation as organizing center of the dynamics: numerical semiglobal results, SIAM J. Appl. Dyn. Syst. 14 (2015) 1130–1164.

[47] D. Ruelle, F. Takens, On the nature of turbulence, Commun. Math. Phys. 20 (1970) 167–192.

[48] K. Saleh, F.O.O. Wagener, Semi-global analysis of periodic and quasi-periodic normal-internal $k:1$ and $k:2$ resonances, Nonlinearity 23 (2010) 2219–2252.

[49] P.H. Steen, S.H. Davis, Quasiperiodic bifurcation in nonlinearly-coupled oscillators near a point of strong resonance, SIAM J. Appl. Math. 42 (1982) 1345–1368.

[50] F. Takens, Introduction to Global Analysis, in: Comm. Math. Inst., vol. 2, Rijksuniversiteit Utrecht, 1973.

[51] R. Vitolo, H.W. Broer, C. Simó, Routes to chaos in the Hopf-saddle-node bifurcation for fixed points of 3D-diffeomorphisms, Nonlinearity 23 (2010) 1919–1947.

[52] D.Yu. Volkov, The Andronov–Hopf bifurcation with 2:1 resonance, J. Math. Sci. 128 (2005) 2831–2834.

[53] F.O.O. Wagener, Semi-local analysis of the $k:1$ and $k:2$ resonances in quasi-periodically forced systems, in: H.W. Broer, B. Krauskopf, G. Vegter (Eds.), Global Analysis of Dynamical Systems. Festschrift Dedicated to Floris Takens for His 60th Birthday, Inst. of Phys., Bristol, 2001, pp. 113–129.

[54] F.O.O. Wagener, A note on Gevrey regular KAM theory and the inverse approximation lemma, Dyn. Syst. 18 (2003) 159–163.

[55] F.O.O. Wagener, A parametrised version of Moser's modifying terms theorem, Discr. Cont. Dyn. Syst., Ser. S 3 (2010) 719–768.